buildings

Article

# The Impact of High-Alkali Biofuel Fly Ash on the Sustainability Parameters of Concrete

**Džigita Nagrockienė *, Ina Pundienė, Loreta Kanapeckienė and Ela Jarmolajeva**

Faculty of Civil Engineering, Vilnius Gediminas Technical University, Saulėtekio Ave. 11, LT-10223 Vilnius, Lithuania; ina.pundiene@vilniustech.lt (I.P.); loreta.kanapeckiene@vilniustech.lt (L.K.); ela.jarmolajeva@vilniustech.lt (E.J.)
* Correspondence: dzigita.nagrockiene@vilniustech.lt

**Abstract:** The results of this research show that high-alkali biofuel fly ash (BFA) had a significant influence on the mechanical characteristics, microstructure, porosity, freezing–thawing cycle resistance, and ASR resistance of cementitious materials. Different amounts of BFA (varying from 0 to 30%) were used as a substitute for cement in concrete mixes. The impact of substituting cement with BFA on the cement hydration products was analysed. Slump behaviour, mechanical properties, water absorption, porosity, freeze–thaw cycles, and ASR resistance were studied. The analysis of the mechanical and physical characteristics of the developed sustainable concrete revealed that a better structure, higher compressive and flexural strength and density values, and better freeze–thaw and ASR resistance as well as lower water absorption values were achieved when as much as fifteen percent of cement was substituted with high-alkali BFA. The calculations indicate that the substitution of cement with different quantities of high-alkalinity BFA (from 0% to 30% BFA) increased the $SiO_2/CaO$ ratio from 0.32 to 0.51 and the $Na_2O$ + $K_2O/CaO$ ratio from 0.02 to 0.067 in the composition. An evident higher quantity of the hydration products, reflected in the reduction of porosity by up to 27%, the improvement in compressive strength by up to 19.3%, and the calculated freeze–thaw resistance value of up to 51.50%, was observed when the $Na_2O$ + $K_2O/CaO$ ratio did not exceed 0.044. The ASR resistance of the concrete improved with the increase in the $Na_2O$ + $K_2O/CaO$ ratio. This study shows that BFA with high alkalinity is beneficial in the development of sustainable building materials.

**Keywords:** fly ash; ASR resistance; freeze–thaw; sustainable concrete



**Citation:** Nagrockienė, D.; Pundienė, I.; Kanapeckienė, L.; Jarmolajeva, E. The Impact of High-Alkali Biofuel Fly Ash on the Sustainability Parameters of Concrete. *Buildings* **2023**, *13*, 3015. https://doi.org/10.3390/buildings13123015

Academic Editor: Ahmed Senouci

Received: 25 October 2023
Revised: 20 November 2023
Accepted: 30 November 2023
Published: 2 December 2023



## 1. Introduction

Biomass is one of the most important renewable energy sources. Burning biomass, which is mostly derived from forests, creates solid waste, like slag and ash, which needs to be managed properly. Both human health and the environment are negatively impacted by fly ash. As biomass fly ash originates from biogenic material, it has a high carbon content and is considered a hard-to-utilize waste [1]. Wood-based biofuels represent about 9% of worldwide energy production [2,3]. With the growing use of biofuel for energy generation, more waste ash is being generated every year. A crucial initial step in solving the world's waste problem is to replace raw materials with waste and use natural resources sustainably. Biofuel combustion ash can be successfully utilized to produce building materials [4]. Due to of its chemical, physical, and morphological properties, biofuel fly ash, as a pozzolanic additive, can be used to substitute part of the cement portion in cementitious materials [5,6]. As pointed out in the literature, various kinds of biomass fly ash derived from waste are also widely utilized in geopolymer concrete, even considering the various other kinds of biomass fly ash available [7].

Ash is currently widely used in geopolymers, but it is not sufficient for complete waste utilization and management. However, the utilization of wood biofuel fly ash in geopolymers is not widespread due to the low aluminium content in and amorphous phase of this kind of ash [8]. Therefore, the utilization of biomass fly ash in cementitious materials is still relevant. Biomass fly ash is mainly used in binder materials, such as Portland cement clinker, in the concrete industry [8]. The possibility of using the biofuel fly ash used in the concrete industry to reduce the $CO_2$ footprint is also important. Studies have demonstrated the potential application of biofuel fly ash as a renewable waste material for cement substitution [9]. Nevertheless, the currently applicable specifications of fly ash exclude biofuel fly ash from being added in concrete because it is not a coal combustion waste. A large number of studies have been conducted on the use of biofuel fly ash (BFA) in concrete or mortar [9–34].

The capacity of BFA to bind with calcium compounds makes it a valuable constituent of cement on par with mineral aggregates. Due to its pozzolanic properties, BFA is used as an active additive to modify the functional properties of a binder [26]. BFA can be applied in the manufacture of concrete mixtures and prefabricated concrete elements [33]. For instance, BFA in porous concrete acts as both a binder and a filler. The developed products with improved technical characteristics are produced at lower cost [23].

BFA incorporated in concrete as a cement substitute may have a significant effect on the fresh and hardened cement paste properties. These properties depend on the burning process, the kind of wood and the pieces of trees turned into biomass, and local operating conditions [11]. The most frequently examined properties of concrete mixtures containing 5–45% BFA by weight of cement are rheological properties, heat of hydration, 7- and 28-day compressive strength, porosity, and capillary absorption. Gabrijel et al. stated that the replacement of up to 15% of cement with very fine BFA accelerated cement hydration and raised the concrete's compressive strength by up to 18%, whereas in samples where cement was substituted with coarser BFA, the heat released more gradually, and the compressive strength decreased by 5%. Although almost no changes were observed in capillary absorption values in samples where up to 45% of cement was substituted with BFA, only the minimum mechanical properties of concrete for use in construction were achieved. The rheological properties of concrete were found to improve when biomass fly ash was used as a filler and as a substitute for fine fillers in concrete [16].

The authors of one study compared mortars modified with BFA and coal combustion waste fly ash and found similar compressive strength values, although their porosity, water absorption, and water vapour permeability were higher [13]. Mortars wherein more cement is replaced with BFA usually have higher water demand and significantly lower compressive strength [12–16,18,34]. Ban and Ramli [22] studied structural concrete wherein certain parts of cement were replaced with BFA and concluded that BFA raised the water requirements and decreased the mechanical strength of the concrete, but it had an insignificant effect on durability and significantly reduced concrete shrinkage. Udoeyo et al. [21] studied the substitution of biofuel fly ash by up to 30% by weight of cement in concrete and observed a significant drop in mechanical strength (from 9% to 38%), especially in the mixtures containing a high amount of BFA. Other authors claim that low amounts of BFA (added at up to 10% by weight of cement) do not change the mechanical properties of mortars.

A significant effect is observed when 20% of cement is substituted with BFA. The compressive strength of mortars modified with BFA can increase even when a small amount of cement is replaced [34]. Rajamma et al. reported a positive influence of biofuel fly ash on the rheological characteristics of cement paste. The researchers observed a higher rate of hydration and a shorter setting time [6]. They observed an increase in both earlier (2- and 7-day) and later (28- and 90-day) strength. It was found that the speed of hydration and the formation of newly created products depend highly on the content of alkali and the W/B ratio in the pastes [31]. Biofuel fly ash with high quantities of alkaline compounds provides extra alkalinity to cement pastes, accelerates the hydration process, intensifies newly created product formation, and consequently increases the mechanical strength of the specimens [25].

Biofuel fly ash in a cement mixture lowers the rate of hydration [29] and thus protects concrete from thermal cracks and stress [30]. Wang et al. [5,13,24] analysed the impact of the amount of BFA added on the properties of cementitious pastes, the mechanical strength of the specimens, and the durability of concrete. They discovered that adding BFA by weight of cement greatly increased the need for water, prolonged the setting time, increased the amount of air-entraining additive required, and decreased the concrete's long-term durability. However, the effect on chloride penetration, early mechanical strength, and resistance to cyclic freezing and thawing was insignificant. The authors of [9] stated that BFA improves the freeze–thaw resistance of concrete.

Wang S. et al. [5] reported that concrete altered with BFA had the same, or even better, longevity and strength characteristics as ordinary fly ash concrete. Teixeira E. R. et al. [25] came to a similar conclusion, stating that concrete that contains BFA has carbonisation resistance similar to that of ordinary fly ash concrete. The addition of fly ash allows for an increase in the chloride resistance of concrete [26] and shrinkage resistance [27] as well as a reduction in water absorption [28]. One review [35] highlighted that the optimal quantity of cement to be substituted depends on the chemical composition of BFA and the quantity of alkali compounds ($K_2O$ and $Na_2O$). As generally indicated in several studies, the content of $K_2O$ and $Na_2O$ in BFA does not exceed 5% [4]. There are few studies in which BFA with higher $K_2O$ and $Na_2O$ content (up to 10–13%) was used. In order to develop the guidelines for using BFA in construction concrete, the interdependency of BFA properties and the characteristics of fresh and hardened concrete should be determined [11]. The data from the reviewed literature leads one to the conclusion that employing BFA as partial substitute for cement in construction materials has the potential to minimize the consumption of natural resources in cement production. BFA is a partially renewable resource: that is why the utilisation of BFA as a partial substitute for cement offers several environmental benefits, including supressing $CO_2$ emissions, reducing fuel consumption, and facilitating BFA's valorisation [36].

Based on the literature review, it can be concluded that the number of available byproducts has been rising recently, and this study's focus is on the binding properties that can be obtained by substituting cement with byproducts. BFA with a high alkali content, varying from 0 to 30%, was studied in order to highlight the possibility of applying such BFA in concrete mixes. However, the effect of highly alkaline BFA on the properties of fresh and hardened cement paste is still insufficiently studied. This study examines the use of high-alkali BFA as a partial cement replacement and its impact on a number of concrete characteristics, including workability, mechanical properties, porosity, structure, durability, and sustainability. The aim of this study is to determine the potential of high-alkali BFA as a material for producing sustainable concrete and to ascertain when it is appropriate to use BFA in place of cement components to lower the cost of concrete.

## 2. Materials and Methods

The tests were performed using CEM I 42.5 R, which satisfies all standards specified in EN 197-1 [37]. Figure 1 illustrates the particle size distribution of Portland cement. The measurements were conducted in the range of 0.10–500 µm. The average size of the particles was 15.05 µm.

BFA collected in electrostatic precipitators of biomass fluidised bed boilers was used to modify fine-grained concrete. To increase the percentage amount of BFA used to replace cement in concrete mix without compromising the properties of the cementitious composite, sieved BFA with a particle size of less than 100 µm was used [10]. The measurement results are presented in Figure 2. The sieved BFA particles were approx. 1.5 times bigger than the cement particles. The distribution of particle size was determined using a Cilas 1090 LD device. Water was used as a dispersion medium. The content of solids in the suspension was 12–14%. The particle size of BFA was measured in the interval of 0.04–100 µm. The average particle size was 23 µm.

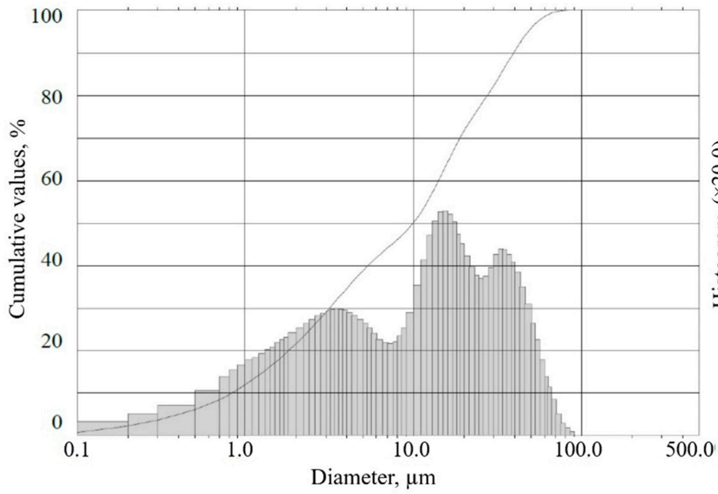


**Figure 1.** Portland cement particle size distribution.

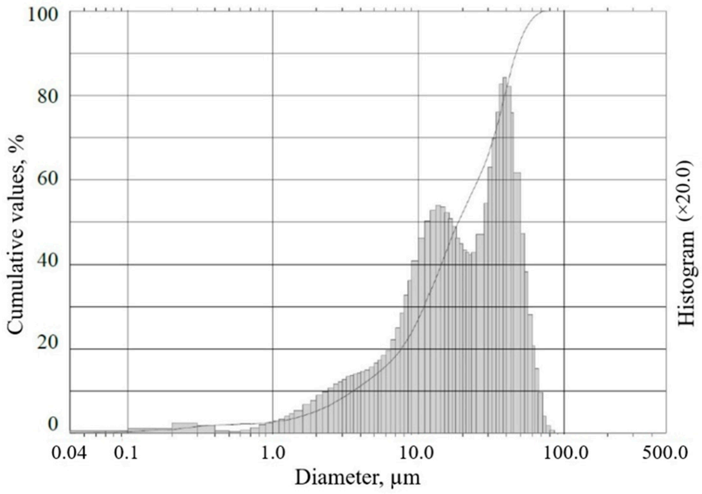


**Figure 2.** Particle size distribution of BFA.

The properties and chemical composition of BFA are presented in Tables 1 and 2. According to research data [6], BFA is characterized by large amounts of $SiO_2$ and CaO and lower amounts of $Al_2O_3$ and $Fe_2O_3$. BFA is expected to participate in pozzolanic and hydraulic reactions because it consists of more than 10% CaO [10,38]. It should be mentioned that the BFA used in this study was highly alkaline, since the total $K_2O$ and $Na_2O$ oxide content was 8.92.

**Table 1.** BFA properties.

| Properties | BFA |
|---|---|
| Particle density, kg/m$^3$ | 2757 |
| Bulk density, kg/m$^3$ | 829 |

Sand in a fraction of 0/4 corresponding to LST EN 12620:2003+A1:2008 requirements [39] was adapted for the tests.

The bulk density of the sand was 1640 kg/m$^3$, and the density of its particles was 2622 kg/m$^3$.

Seven batches of sustainable concrete compositions were prepared. Mixing procedure employed is as follows: dry components, i.e., cement, BFA, and sand, were mixed for 5 min; then, water was added, and the blend mixed again for 5 min.

**Table 2.** Chemical composition of Portland cement and BFA.

| Chemical Composition of BFA, Mass % | | | | | | | | | | |
|---|---|---|---|---|---|---|---|---|---|---|
| $SiO_2$ | $Al_2O_3$ | $Fe_2O_3$ | CaO | $K_2O$ | $SO_3$ | $Na_2O$ | $P_2O_5$ | MgO | $MnO_2$ | Cl |
| 41.93 | 2.70 | 1.91 | 30.3 | 8.43 | 4.95 | 0.49 | 4.75 | 3.6 | 0.59 | 0.38 |
| Chemical composition of Portland cement, mass % | | | | | | | | | | |
| 21.76 | 6.12 | 3.37 | 63.5 | 1.0 | 0.8 | 0.3 | - | 3.15 | - | - |

The batches differed in terms of the content of BFA in the concrete mixture, which ranged from 0% to 30% by weight of cement substituted. BFA was added into the mixture in 0; 5; 10; 15; 20; 25; and 30% portions by weight of cement. Compositions of concrete mixtures are presented in Table 3.

**Table 3.** Concrete compositions, %, and $SiO_2/CaO$, $Na_2O + K_2O/CaO$, and $Al_2O_3/SiO_2$ ratios in the cementitious matrix (cement and BFA).

| Composition Designation | CEM I, % | BFA Content, % Cement | $SiO_2/CaO$ | $Na_2O + K_2O/CaO$ | $Al_2O_3/SiO_2$ | Sand, % | BFA, % | V/R |
|---|---|---|---|---|---|---|---|---|
| I | 30.77 | 0 | 0.320 | 0.020 | 0.294 | 69.23 | 0 | 0.47 |
| II | 29.23 | 5 | 0.353 | 0.027 | 0.276 | 69.23 | 1.54 | 0.47 |
| III | 27.69 | 10 | 0.380 | 0.034 | 0.259 | 69.23 | 3.08 | 0.47 |
| IV | 26.15 | 15 | 0.409 | 0.043 | 0.241 | 69.23 | 4.62 | 0.47 |
| V | 24.62 | 20 | 0.440 | 0.050 | 0.223 | 69.23 | 6.15 | 0.47 |
| VI | 23.08 | 25 | 0.471 | 0.058 | 0.206 | 69.23 | 7.69 | 0.47 |
| VII | 21.54 | 30 | 0.506 | 0.066 | 0.188 | 69.23 | 9.23 | 0.47 |

Using a Bruker X-ray S8 Tiger WD X-ray fluorescence spectrometer, BFA was chemically analysed. Rh target X-ray tube was used, and an anode voltage up to 60 kV and a current (I) up to 130 mA were employed. Pressed samples were measured in a helium environment. The measurements were performed using the SPECTRA Plus QUANT EX-PRESS technique.

The structure of BFA was tested using a scanning electron microscope (SEM JEOL JSM-7600F). The microscopy parameters were as follows: the voltage applied was 10 kV and 20 kV, and the distance to the specimen surface ranged from 7 to 10 mm.

The properties of the specimens tested were determined according to applicable standards: LST EN 12350-5:2019 [40] for the flow of the mixtures, LST EN 12390-7:2019 [41] for the density of hardened sustainable concrete, LST EN 12390-3:2019 [42] for compressive strength, and LST EN 12390-5:2019 [43] for flexural strength.

Ultrasonic pulse velocity (UPV) test was carried out following the recommendations of standard LST EN 12504-4 [44].

The durability of sustainable concrete predicted according to freeze–thaw cycles was measured based on porosity parameters. Frost resistance factor $K_F$ was calculated based on the assumption that concrete is frost-resistant when the volume of closed pores is higher than the increased volume of frozen water in capillary pores. Frost resistance factor $K_F$ was calculated using the following equation:

$$K_F = \frac{P_u}{0.09\,P_a} \tag{1}$$

where $P_u$ is closed porosity, and $P_a$ is open porosity.

Using the known value of frost resistance factor $K_F$, the resistance of concrete to freezing and thawing cycles can be predicted from the function of freeze–thaw resistance and frost resistance factor $K_F$. Porosities were determined using Scheikins theory [45].

ASR resistance of sustainable concrete was determined using the RILEM AAR-2 method. The test lasted fifty-six days. The cured samples were kept in 1 M NaOH solution at a temperature of 80 °C for fifty-six days. On day 56, the expansion of the specimens was tested. ASTM C 441 indicates that the expansion limit was 0.1%.

## 3. Results and Discussion

### *3.1. Parameters of BFA*

Figure 3 presents the BFA X-ray structural analysis results. The X-ray image shows that quartz ($SiO_2$), which is present in 75% of the sample, is the predominant mineral. $SiO_2$ usually forms during the burning of biomass at high temperatures [46]. Calcium oxide (CaO) is the second mineral prevailing in fly ash by content (12.8%). Other minerals identified in the X-ray analysis were calcite and portlandite, present at 7.0% and 2.8%, respectively. Similarly, the same minerals, but in different amounts, were found in BFA by other researchers [47,48].

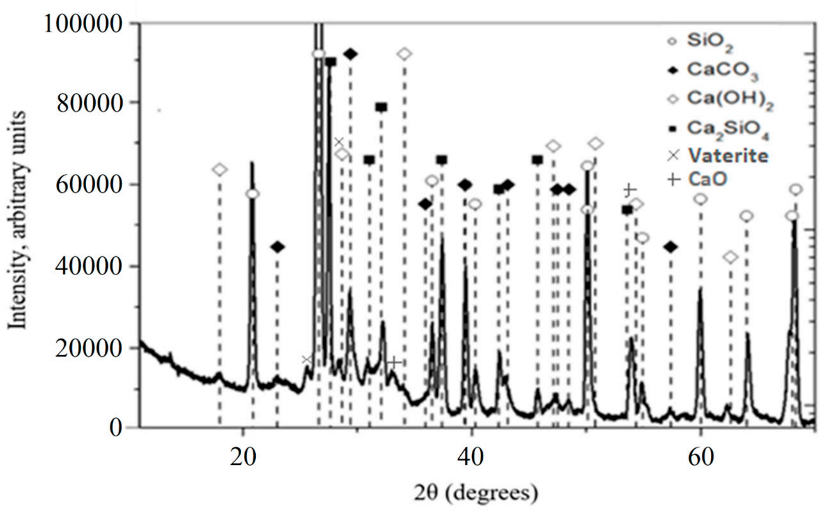


**Figure 3.** X-ray diagram of BFA.

The results of the BFA analyses performed using SEM are presented in Figure 4. Figure 4 shows a great variety of BFA particle forms and sizes; there are also visible soot particles or pieces of unburned wood.

BFA was found to have the pozzolanic activity of 350 mg of CaO/g ash. It was discovered that BFA has a significantly larger amount of $SiO_2$, which interacts with the $Ca(OH)_2$ in the cementitious system to create more hydration products. The mechanical and physical characteristics of sustainable concrete are enhanced by these reaction products. After numerous experiments, Quarcioni, a researcher, found the following pozzolanic activity values of BFA: 279 mg of CaO/g for sugar cane, 622 mg of CaO/g for rice husk, 269 mg of CaO/g for wood, 622 mg of CaO/g for metakaolin, and 755 mg of CaO/g for silica fume [49].

A thermogravimetric examination of BFA revealed (Figure 5) an endothermic reaction in the 335–412 °C temperature interval, where portlandite decomposition takes place. Another effect of an endothermic reaction, namely, the decomposition of vaterite, was observed in the temperature interval of 500–740 °C. The mass loss during this reaction was 7.81%; decomposition of calcite occurs at a temperature interval of 740–800 °C. The total mass loss was 12.34% [50].

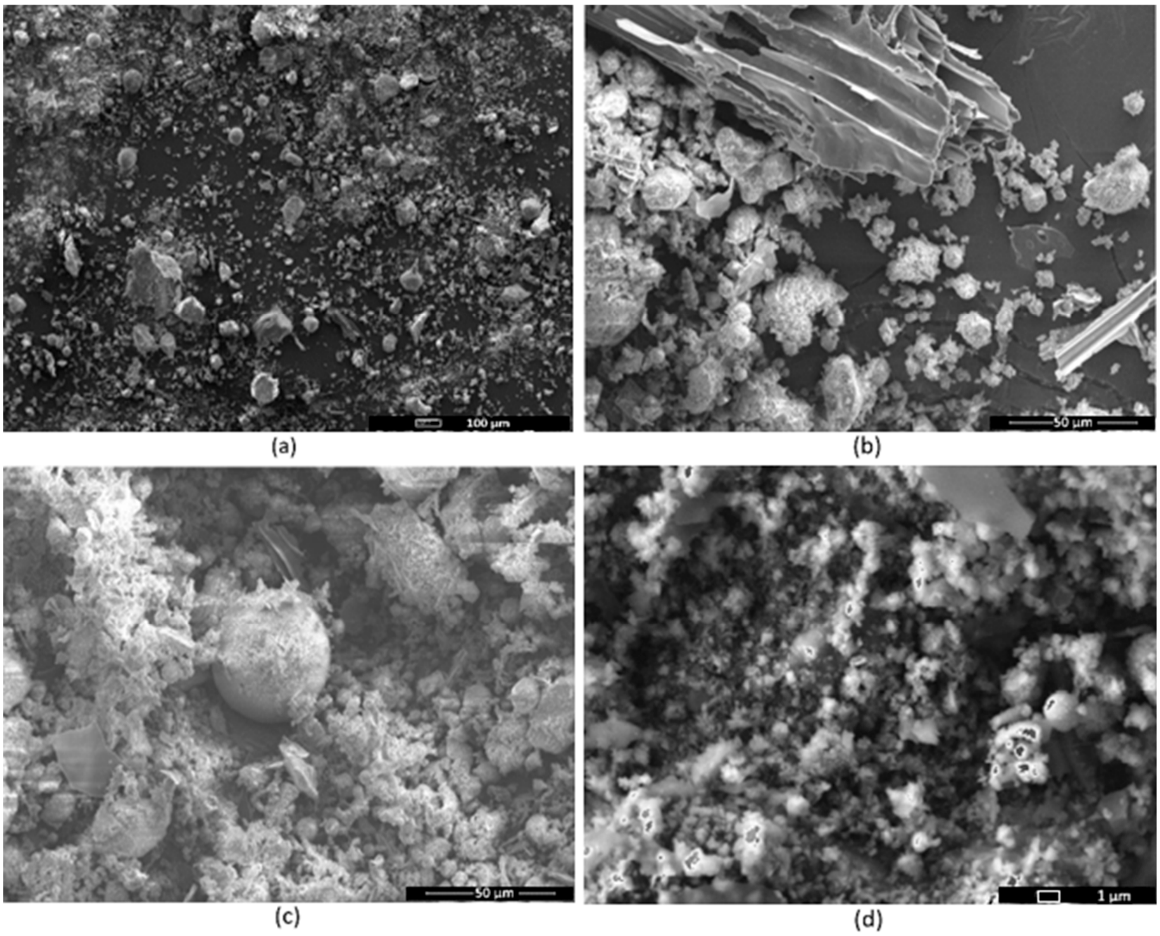


**Figure 4.** Microstructure of BFA: (**a**) 200× magnification; (**b**,**c**) 1000× magnification; (**d**) 10,020× magnification.

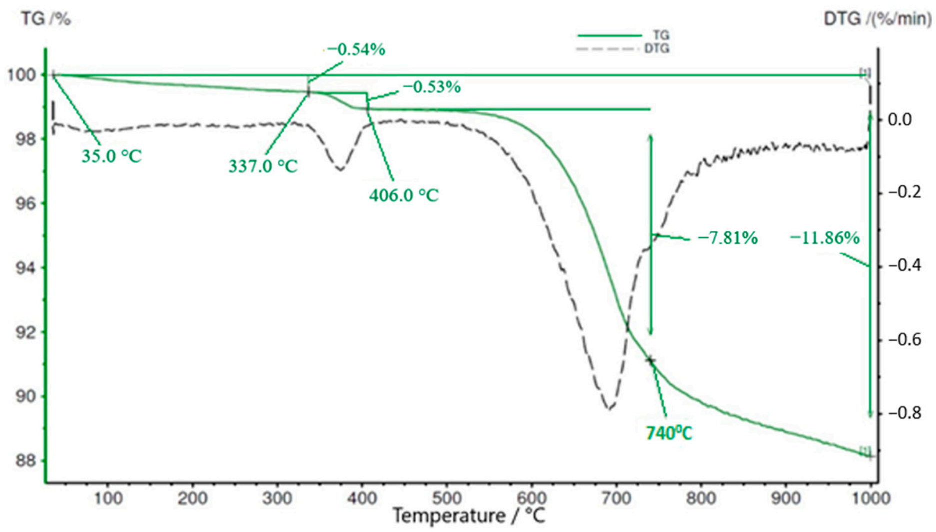


**Figure 5.** Thermal images of BFA.

*3.2. X-ray of BFA Modified Hardened Cement Paste*

X-ray tests were conducted on hardened cement paste containing 0%, 15%, and 30% BFA by weight of cement after 28 days of curing. The test results are shown in Figure 6.

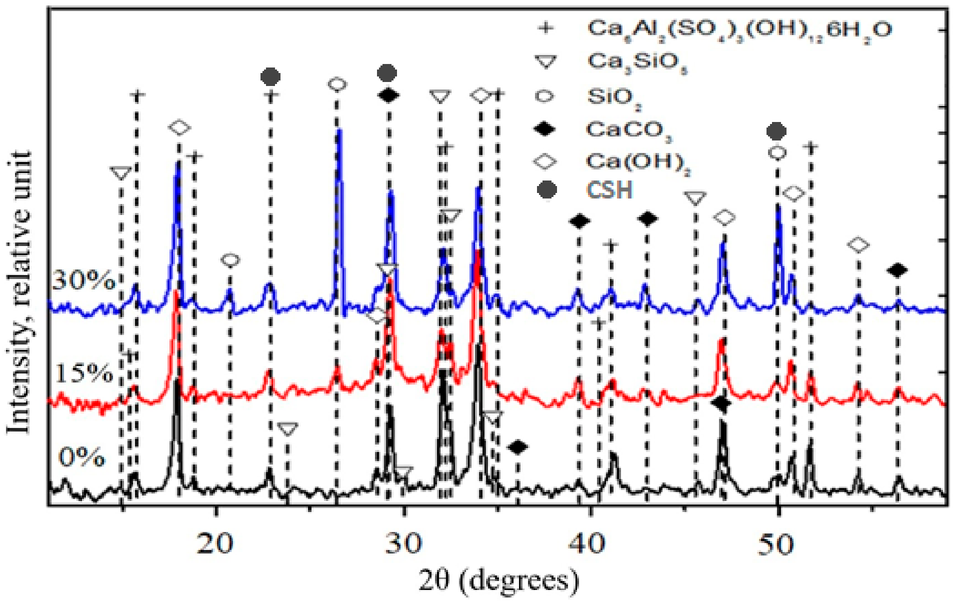


**Figure 6.** X-ray image of hardened cement pastes with different BFA proportions.

The tests showed that all the specimens contained portlandite, calcite, ettringite, and CSHs as well as non-reacted cement minerals. Only the amounts of the minerals identified in the specimens differed. The samples in which BFA substituted for 15% and 30% of cement showed a reduction in the amounts of portlandite and ettringite. The decrease in portlandite can be associated with a decrease in the amount of cement and, accordingly, a significant increase in the $SiO_2/CaO$ ratio (from 0.32 to 0.51) in the cement matrix (Table 3).

The decrease in ettringite can be explained both by an increase in the $SiO_2/CaO$ ratio and a significant reduction in the $Al_2O_3/SiO_2$ ratio (from 0.294 to 1.88) when the amount of $Al_2O_3$ was insufficient for significant ettringite formation. At the same time, a more intense formation of calcium hydrosilicates (CSHs) was observed in the cement matrix with BFA. Due to the presence of active $SiO_2$ in BFA, which participates in the reaction with portlandite, calcium hydrosilicates (CSHs) are formed. It is known that alkali compounds, which are present in large quantities in BFA, promote the hydration of cement minerals and the release of Ca ions into a solution [51].

Therefore, despite the decrease in the amount of cement in the cement matrix, a noticeable number of CSHs were formed. Other researchers [52,53] also reported higher consumption of portlandite in the presence of Si-rich additives. When more cement is replaced with BFA, the $Na_2O + K_2O/CaO$ ratio increases threefold (from 0.02 to 0.067). The calculated $Na_2O + K_2O/CaO$ ratio in the cement matrix is based on this assumption. These results indicate that more calcium ions participle in the CSH crystallisation process in cement matrix with BFA [54,55]. The pozzolanic activity of BFA can promote the crystallisation of CSHs [56].

The peaks of quartz are the most intense in the cement matrix with 30% BFA replacing cement, as the calculated $SiO_2/CaO$ ratio was the highest in this specimen (Table 3).

The results show that the samples modified with BFA have a higher level of alkalinity, and perhaps more CSHs are formed in the pozzolanic reaction of BFA. According to the authors of [51], a decrease in portlandite can be seen in such cementitious samples in comparison to control samples.

### *3.3. Thermogravimetric Analysis of BFA-Modified Hardened Cement Paste*

After 28 days of curing, TG/DTG analysis of the samples of compositions I, IV, and VII was performed (Figures 7–9). The TG/DTG curves show three main effects of the endothermic reaction, during which the samples experienced significant weight loss. The mass loss in the temperature range 400–450 °C was caused by the release of water [57], as ettringite, calcium hydroaluminates, monocarboaluminates, and CSH lose hydrated water [58,59]. The first endothermic effects in the temperature range of 90–200 °C could be mainly attributed to the decomposition of ettringite (90–150 °C) and the decomposition of calcium silicate hydrates (which generally takes place in the temperature range of 160–200 °C). The decomposition of portlandite takes place between 400 and 500 °C, while the decomposition of carbonates occurs above 550 °C [60].

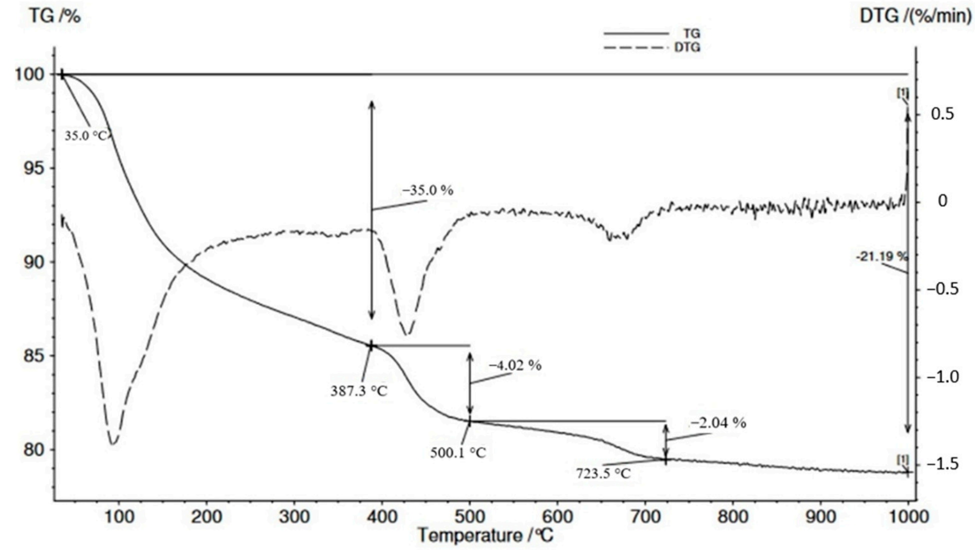


**Figure 7.** Thermal images of cement paste I sample.

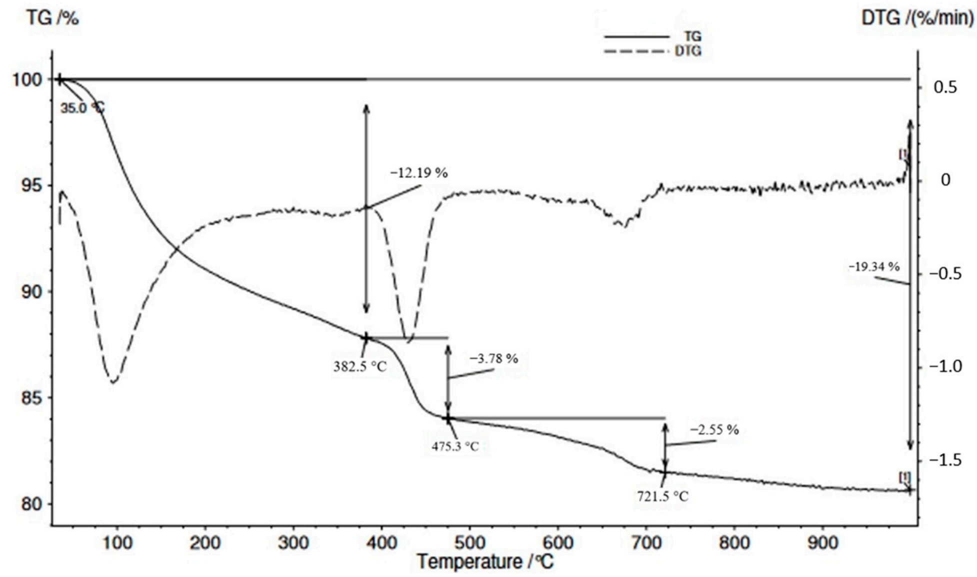


**Figure 8.** Thermal images of cement paste IV sample.

Table 4 presents the weight loss of the samples during heating in various temperature ranges as determined using the DTG method. The overall weight loss in the specimens modified with BFA was 2.3% to 3.3% higher than that in the control specimen. Compared to the control sample, the weight loss in the samples modified with BFA was 2.3% to 3.3% higher.

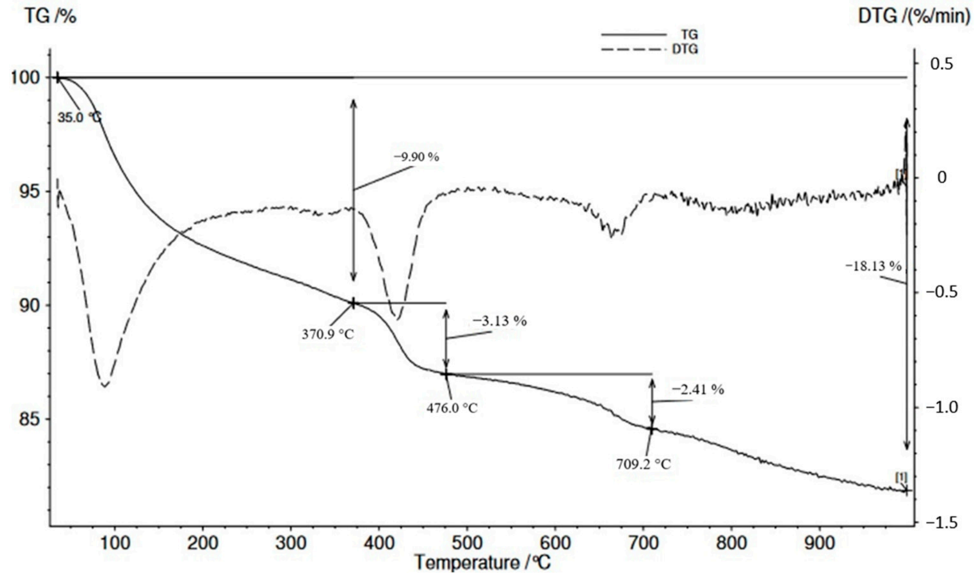


**Figure 9.** Thermal images of cement paste VII sample.

**Table 4.** The weight loss by percentage in samples of different composition determined during the DTG test.

| Sample Designation | Weight Loss, %, in the Temperature Range Up to the Following Values | | | | | Cement Content in Composition, % |
|---|---|---|---|---|---|---|
| | 150 °C | 200 °C | 500 °C | 750 °C | 1000 °C | |
| I | 9.1 | 11.7 | 4.02 | 2.04 | 21.19 | 100 |
| IV | 7.0 | 10.3 | 3.78 | 2.55 | 19.34 | 85 |
| VII | 5.8 | 8.1 | 3.13 | 2.41 | 18.13 | 70 |

The weight loss of the samples of tested compositions decreased from 9.1% to 5.8% at temperatures below 150 °C. Presumably, the mass loss related to ettringite decomposition decreases at the temperature interval indicated above. It can be seen that the decrease in ettringite formation reached 36%, compared to control specimen. This could be linked to the rising $SiO_2/CaO$ ratio and the decrease in $Al_2O_3/SiO_2$ [61]. These findings correspond to the data presented in some studies as well as the XRD results (Figure 6).

Within the temperature range of 160–200 °C, bound water is released during the CSHs' decomposition. In this case, the DTG analysis results confirm the XRD results and show that the substitution of 15% of cement with BFA decreased CSH formation by only 12%, while the substitution of 30% of cement with BFA decreased CSH formation up to 31%, compared to the control sample. Such trends in the formation of CSHs suggest that the $Na_2O + K_2O/CaO$ ratio of 0.043 had a positive effect on the formation of CSHs in the sample. The decomposition of portlandite is directly related to the replacement of cement with BFA [17]. With a higher amount of BFA used as a substitute for cement, the weight loss decreased from 4.02% to 3.13%.

The results clearly show that the partial substitution of cement with pozzolanic additives accelerates portlandite consumption and CSH development [62]. In the process of carbonate decomposition, the control sample lost 2.04% of its weight. The amount of $CaCO_3$ in the specimens was also affected by the amount of cement present in the system, and it tended to decline as the samples produced continuously less $Ca(OH)_2$, allowing it to react with atmospheric $CO_2$. The presence of BFA increased the $CaCO_3$ amount and possible additional formations. It is known that the quantity of pozzolanic additives in a sample has a significant impact on the amount of $CaCO_3$ [63].

The comparison with the control composition showed that even with a lower cement amount in the composition, pozzolanic additives, such as BFA, support higher levels of cement hydration and CSH creation. BFA hinders the formation of ettringite, but when the $SiO_2/CaO$ ratio varies between 0.32 and 0.41 and the $Na_2O + K_2O/CaO$ ratio varies between 0.032 and 0.043, it promotes CSH formation to a certain extent.

### *3.4. SEM Analysis of BFA-Modified Hardened Cement Paste*

XRD tests of the cement matrix were supplemented with microstructure analysis. The microstructure was analysed with SEM at 10,000× magnification. Figures 10–12 show SEM images of hardened cement paste containing different amounts of LMP ash replacing cement. Portlandite and $CaCO_3$ clusters, calcium hydrosilicates (CSHs) and well-crystallized coarse ettringite (AFt) needles are shown in Figure 10. Large accumulations of CSHs are shown in the specimen where 15% of cement was replaced with BFA (Figure 11). Portlandite and ettringite can also be observed.

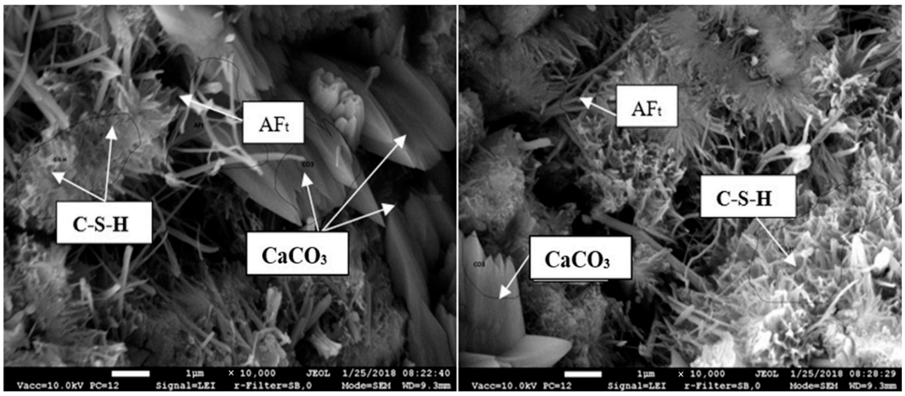


**Figure 10.** Microstructure of the BFA-free hardened cement matrix.

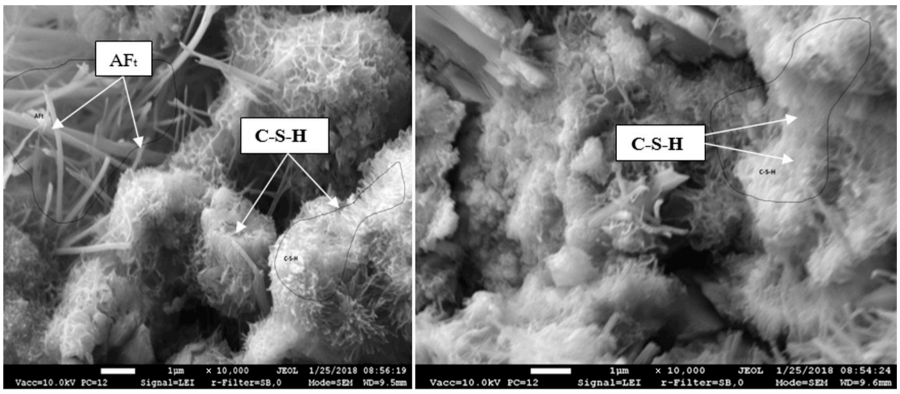


**Figure 11.** Hardened cement matrix microstructure with 15% of cement substituted with BFA.

Less-crystallized ettringite and large portlandite crystals, which are formed in water-filled pores, are shown in the cement matrix, where 30% of cement was substituted with BFA (Figure 12). The same CSHs were identified, but their accumulations are not as pronounced as those in the specimen where 15% of cement was replaced by BFA.

The SEM analysis results confirm the XRD and DTA analyses results and that the ratio of alkali, calcium, silicon, and aluminium greatly influences the ratio of hydrates formed as well as the cement hydration process.

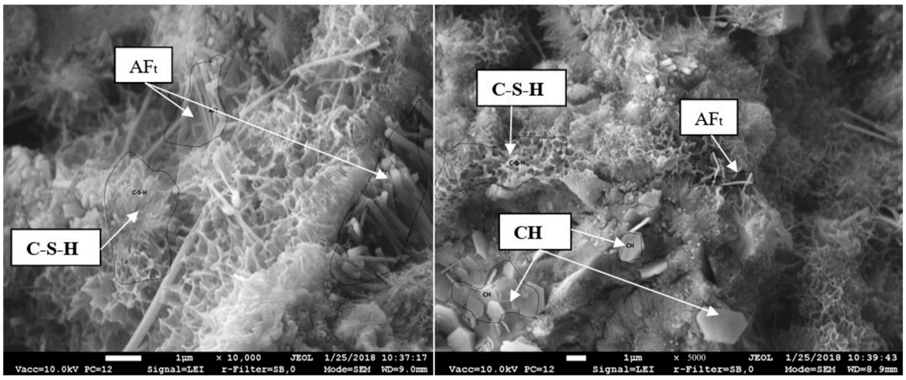


**Figure 12.** Hardened cement matrix microstructure with 30% of cement substituted with BFA.

### 3.5. Properties of Concrete

The workability tests revealed that a higher amount of BFA in the mixture reduced the slumps from 171 to 130 mm. Although the median size of the particles of BFA is greater than the size of cement particles, BFA has a lower bulk density than the density of cement. BFA fine particles have a large specific surface area, and this induces high water requirements. As the water-to-binder ratio was kept constant, the slump started decreasing. The same tendencies were reported in [64,65]. The compositions of the concrete mixtures are presented in Table 5.

**Table 5.** Slump flow of concrete mixture (mm).

| Batches | I | II | III | IV | V | VI | VII |
|---|---|---|---|---|---|---|---|
| Slump flow, mm | 171 | 170 | 169 | 166 | 165 | 140 | 130 |

The results of the hardened cement paste density and ultrasonic pulse velocity tests are presented in Figure 13. The measured density of the control specimen was 2215 kg/m$^3$. The highest densities of 2230 kg/m$^3$ and 2223 kg/m$^3$ were found in the concrete samples wherein 10% and 15% proportions of cement were substituted with BFA. Such an insignificant increase in density can be explained by the cement dilution effect when a denser structure is formed as a result of different particle sizes, better particle size distribution, and the development of new products [22].

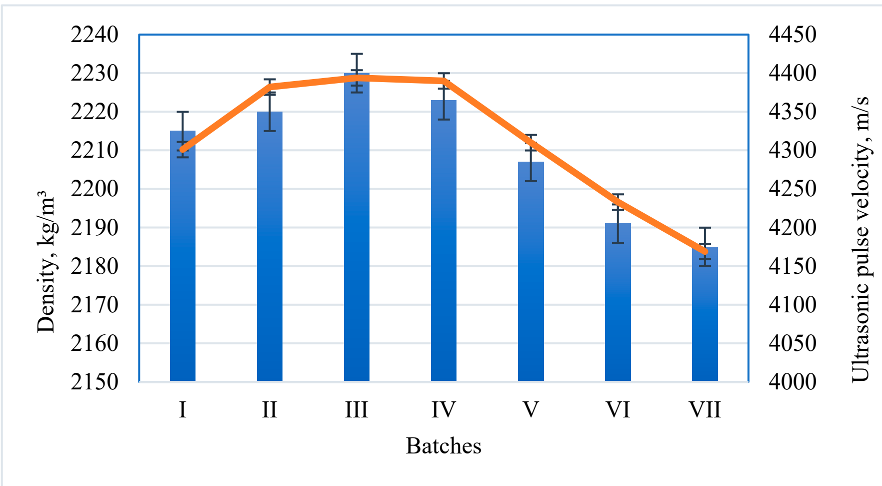


**Figure 13.** Density and UPV of sustainable concrete with BFA.

However, the density of concrete started decreasing when a cement portion of more than 15% was substituted with BFA. The specimen wherein 30% of cement was substituted with BFA had the lowest density. The tests showed that 20% of cement can be substituted with BFA without a critical reduction in concrete density.

Figure 13 illustrates the results of the UPV test. The control sample had a UPV value of 4301 m/s. The samples wherein 10%, 15%, and 20% of cement was substituted with BFA had the highest UPV values of 4394 m/s, 4390 m/s, and 4310 m/s, respectively. These tests also confirm that a better concrete structure is formed when 5% to 20% of cement is substituted with BFA.

The flexural strength tests showed that the concrete samples wherein 10% of cement was substituted with BFA had the highest flexural strength of 7.4 MPa. The control samples had a flexural strength of 6.9 MPa (Figure 14), which increased by 7.25% when 10% of cement was substituted with BFA. The results presented in Figure 14 show that with the increase in the BFA amount by up to 20%, the flexural strength reaches the value of control sample's strength.

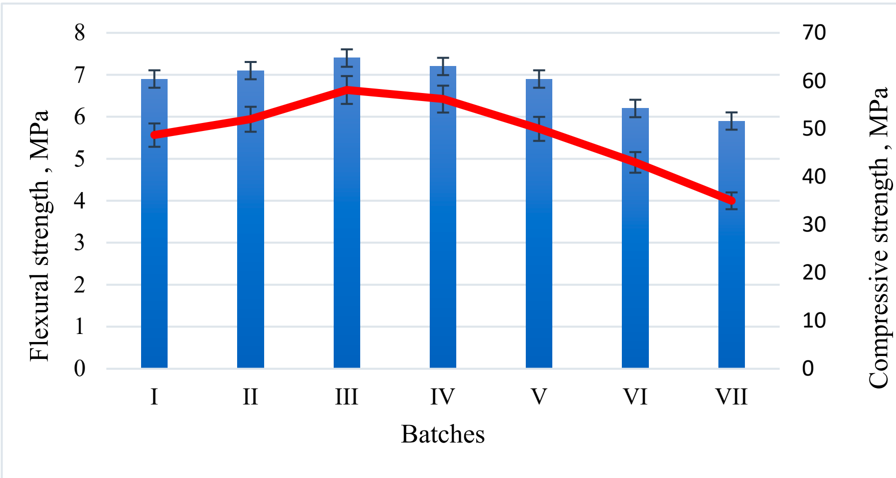


**Figure 14.** BFA-modified sustainable concrete's flexural and compressive strengths.

This result contradicts the results of a study [16] wherein cement was replaced with up to 30% of BFA. The researchers found that with the growth in the BFA content in the cement matrix, the flexural and compressive strength dropped. It is worth mentioning that the above-mentioned study used fly ash with low alkali content (up to 3.5%). When the BFA amount was increased to 30%, the flexural strength value reduced to 5.9 MPa, i.e., 14.5%, compared to the control specimen.

The compressive strength values are presented in Figure 14. The compressive strength of the control sample was 48.7 MPa. A 19.3% growth in compressive strength to a maximum value of 58.1 MPa was observed in the samples with 10% BFA by weight replacing cement. With an increase in the BFA amount in the concrete specimens up to 20%, the compressive strength still remains higher than that of the control samples and reaches 50 MPa. It is important to note that the compressive strength results obtained in this study are up to 20–30% higher than those indicated by another author who used low-alkali BFA as a substitute for cement [13,35,47] and they are up to 10–20% higher than those indicated by another author who used ash with low alkaline content. The compressive strength started decreasing with the increase in the BFA amount to 30% and then dropped to 35 MPa. These results indicate that BFA may give extra alkalinity to the pastes. When the $SiO_2/CaO$ ratio varies in the range of 0.32–0.41 and the $Na_2O + K_2O/CaO$ ratio does not exceed 0.043, the alkalinity factor is beneficial for the growth in the compressive strength of cement-based materials. Similar observations were made by other authors [25].

### *3.6. Durability Analysis*

The results of water absorption tests conducted using completely dry specimens of sustainable concrete are presented in Figure 15. When up to 20% of cement was substituted with BFA, the water absorption of the samples tended to reduce. However, when more cement (up to 30%) was substituted with BFA, water absorption increased. These results correlate with the density results (Figure 13) and indicate that at a lower BFA content, the structure of concrete is denser due to better particle size distribution.

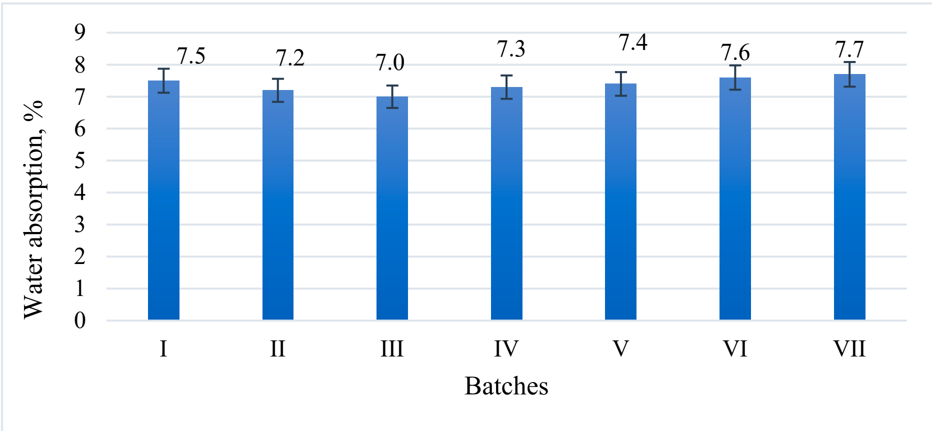


**Figure 15.** Water absorption of sustainable concrete modified with BFA.

The lowest water absorption was observed in the batch of samples wherein 5% and 10% of cement was substituted with BFA. In contrast to the control sample, there was a 4–6% reduction in water absorption. With a further increase in BFA by weight in the cement, the water absorption increased. However, the water absorption of the samples wherein 20% of cement was substituted with BFA remained lower than that of the control sample. The same trends were observed in another study [15,66].

Open, closed, and total porosity values were determined by testing the specimens. Figure 16 presents the obtained data.

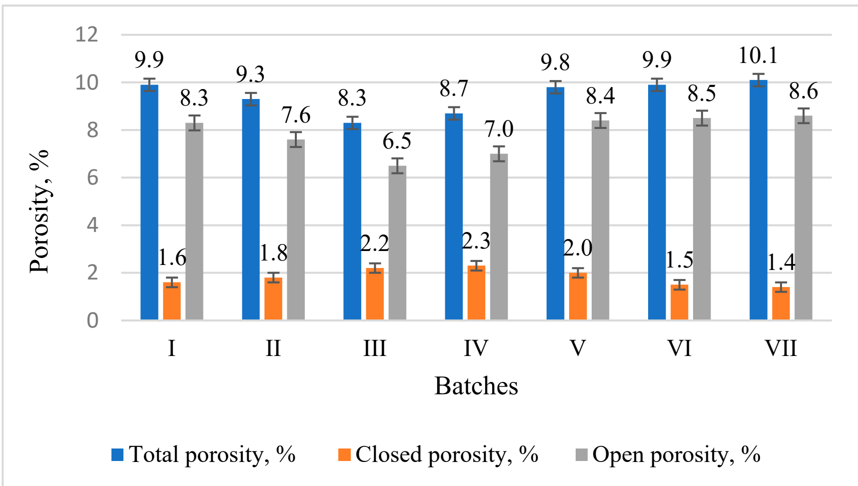


**Figure 16.** Porosity of sustainable concrete modified with BFA.

The closed porosity was observed to increase from 1.6% to 2.3% with the increase in cement substitution with BFA up to 15%. This trend corresponds to the density and water absorption results of the specimens tested. Researchers have found [67] that concrete specimens modified with BFA develop a denser microstructure through a significant reduction in pores and thus have greater mechanical strength (compressive, tensile, and flexural) and a higher modulus of elasticity. According to the authors of [48], a lower content of BFA may promote the development of closed pores in the structure due to a more intensive hydration process and the filling of pores with newly formed products. BFA-modified concrete can have a denser microstructure and significantly fewer pores and thus greater mechanical strength (compressive, tensile, and flexural) and a higher modulus of elasticity.

When up to 20% of cement was substituted with BFA [48], the closed porosity reached 2.0% but remained higher than that of the control specimen. The smallest closed porosity readings were found in the samples wherein 25% and 30% of cement were substituted with BFA.

The open porosity of the specimens reduced and reached 6.5–7.0% when the content of cement substituted with BFA was increased to 10–15%. When cement replacement reached 30%, the open porosity of the specimens increased to 8.6%. The authors of one study noted [51] that the inclusion of BFA in the mortar compositions tested influenced the pore distribution significantly. The study presented in [47], which was carried out with similar compositions, showed that the sample's total porosity reached 21–26% when less-alkaline BFA was used for the study. This comparison illustrates the significance of alkaline content in the used BFA. With the increase in cement substitution with BFA, the volume of 0.01 mm–0.1 mm and 0.1 mm–1 mm diameter pores increased to more than twice that of the control samples. A highly variable pozzolanic material particle form may increase the number of small pores and alter samples' total porosity according to the researchers who authored [25].

The lowest total porosity was found in the samples wherein 10–15% of cement was substituted with BFA as a result of the ratio of closed and open pores.

### *3.7. Analysis and Forecast of Sustainability of Concrete Samples Modified with BFA*

Results on the freeze–thaw resistance of concrete modified with BFA were reported only in a few investigations [20,25]. These results demonstrated that the presence of BFA does not influence the decrease in specimen mass because of higher possible air entrainment in the specimens with BFA [68].

The frost resistance criterion was determined according to the research methodology presented in [50] to forecast the durability of concrete, i.e., resistance to cyclic freezing and thawing. The frost resistance criterion is presented in Table 6, and the predicted resistance to cyclic freezing and thawing is provided in Figure 17.

**Table 6.** Frost resistance criterion of sustainable concrete.

| Batches | I | II | III | IV | V | VI | VI |
|---|---|---|---|---|---|---|---|
| Frost resistance criterion | 2.10 | 2.48 | 3.07 | 2.69 | 2.11 | 1.98 | 1.80 |

Frost resistance is largely determined by porosity, i.e., pore type, the pores' sizes and distribution, and the structure of the pore space of the material [69]. The authors of [70] state that pores are traditionally categorized by their diameter into three categories: reserve (more than 200 microns, in which water is not retained), hazardous (from 0.1 to 200 microns, in which water freezes inside), and safe (less than 0.1 microns, in which water does not enter and hence does not freeze inside during the winter). The addition of fly ash can increase frost resistance because it introduces a growing number of pores of 10–100 μm in diameter and open micropores less than 1 μm in diameter. In [71], it was demonstrated that the level of mechanical degradation increased with the increase in pore volume above 20 nm.

The concrete incorporating 20% BFA had less permeability and, therefore, had superb resistance to cyclic freezing and thawing (the samples withstood 300 cycles of freezing and thawing at temperatures ranging from 18 to +4 °C and de-icing salt scaling deterioration) [72].

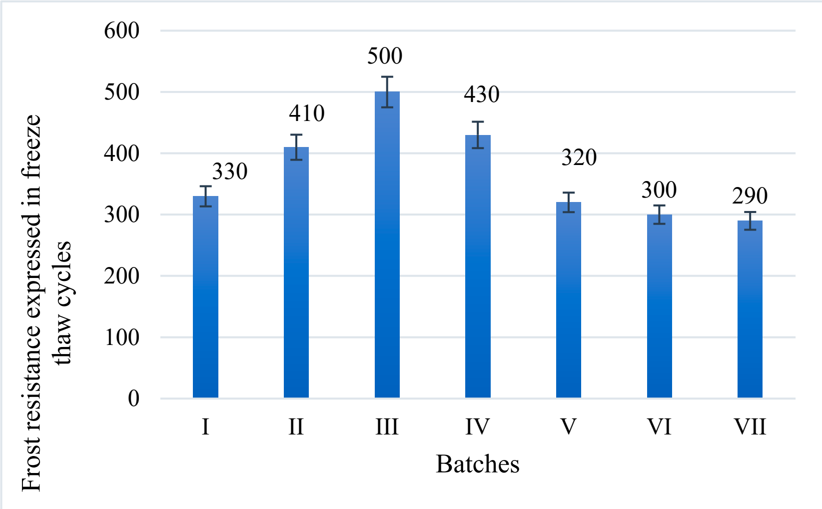


**Figure 17.** Frost resistance in a number of freezethaw cycles of sustainable concrete modified with BFA.

The porosity tests showed that the closed porosity of the specimens increased when the $SiO_2/CaO$ ratio varied in the range of 0.32–0.41, but the $Na_2O + K_2O/CaO$ ratio did not exceed 0.043. These findings correspond to the frost resistance criterion calculation results. When the $Na_2O + K_2O/CaO$ ratio in the composition did not exceed 0.043, the frost resistance criterion assumed values of 2.48, 3.07, 2.69, and 2.11. These results show that the samples wherein 10% of cement was substituted with BFA have a frost resistance criterion value that is 46.1% higher than the value of the control samples.

In the case wherein the proportion of BFA was increased to 20%, the frost resistance criterion value approached the value of the control samples. Authors have also noted [73] the importance of better Ca/Si and Na/Si ratios for improving the frost resistance of concrete. Frost resistance improves with a higher Na/Si ratio. The effect of the $SiO_2/CaO$ and $Na_2O + K_2O/CaO$ ratios is also reflected in the number of calculated freeze–thaw cycles (Figure 17). Samples of Batch III were expected to withstand the highest number of freeze–thaw cycles because the numbers of cycles they withstood was 51.5% higher in comparison to the control samples. When the percentage of BFA was increased to 15%, the samples of Batch IV still had a 30.3% higher frost resistance value compared to the control samples. When 20% of cement was substituted with BFA, the number of freeze–thaw cycles withstood by the test samples became equal to the number of cycles withstood by the control samples. The frost resistance started decreasing with a further increase in fly ash content.

The alkali–silica reaction (ASR) is known to cause numerous forms of damage in concrete structures when OH ions react with the alkali ions (K and Na) present in an interstitial solution of cementitious materials in humid conditions. The result of this interaction is the creation of a hygroscopic gel. This gel absorbs water and expands, thus leading to the cracking of concrete. As a result, concrete's durability and mechanical qualities decline [10,74,75]. The purpose of this research was to analyse the effect of the substitution of cement with highly alkaline BFA on the ASR resistance of concrete. The ASR resistance test results are shown in Figure 18; these were obtained after the samples were stored for 56 days in a 1 M NaOH solution at 80 °C.

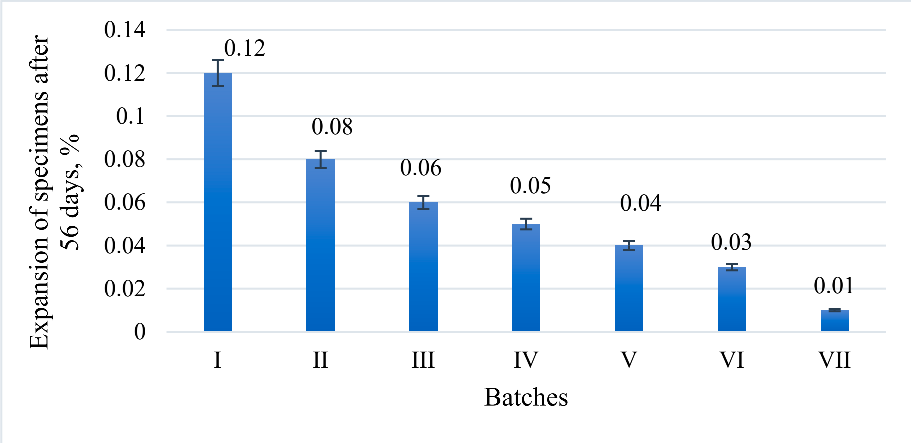


**Figure 18.** Expansion of BFA-modified durable concrete.

The control sample underwent an expansion of 0.12%. The expansion began to decrease when the BFA amount increased. When 5% of cement was substituted with BFA, the expansion of the specimen was 0.08%; at 10% replacement, the expansion was 0.06%; at 15% replacement, the expansion was 0.05%; at 20% replacement, the expansion was 0.04%; at 25% replacement, the expansion was 0.03%; and at 30% replacement, the expansion was 0.01%. The results obtained using the ASTM C 441 test method indicated that after 56 days, the critical expansion limit was 0.1%. It was clearly seen that with a higher BFA content in the mixture, the expansion of the specimens decreased. The results of our study are confirmed by other studies [10], the main purpose of which was to determine BFA's tolerance to ASR damage. The researchers investigated cement-based composites wherein 20% and 30% proportions of cement were substituted with BFA. Visual inspection of the samples showed that the samples consisting of 20% and 30% BFA resisted ASR. With the growth in the cement substitution level, a significant reduction in the expansion of the samples was estimated. Additionally, it was concluded that using BFA as a cement substitute mitigates the damaging effect of ASR even better than coal fly ash.

The aforementioned result was achieved because BFA is more alkaline than coal fly ash [5,76]. These findings further confirm that BFA with higher alkalinity has a greater potential to be utilised in construction materials. In general, it can be concluded that higher BFA substitution levels in compositions lead to the production of more ASR-resistant concrete.

## 4. Conclusions

This study revealed several key aspects of the sustainability of concrete wherein cement was substituted with high-alkali BFA: strength, porosity, and resistance to cyclic freezing and thawing and to ASR.

The following conclusions were drawn regarding the level of cement substitution with BFA in the concrete composition and the $Na_2O + K_2O/CaO$, $SiO_2/CaO$, and $Al_2O_3/SiO_2$ ratios:

1. The chemical analysis and fineness tests of BFA revealed that $SiO_2$, CaO, and $K_2O$ are the main chemical components of BFA. $SO_3$, $P_2O_5$, and MgO are present in lower amounts, and the amounts of other components are not significant. BFA has an average particle size of 23 µm. The pozzolanic activity of BFA was found to be 350 mg of CaO/g ash.
2. With a significant increase in the $SiO_2/CaO$ ratio (from 0.32 to 0.51) due to cement substitution with up to 30% of BFA, the crystallisation of portlandite and ettringite decreased. The decrease in ettringite can be influenced by the $Al_2O_3$ amount in the cement matrix. With the increase in cement substitution with BFA up to 30%, the $Al_2O_3/SiO_2$ ratio decreased from 0.294 to 1.88.
3. The pozzolanic nature of BFA and its numerous alkaline compounds ensured the crystallisation of CSHs in the cement matrix. BFA decreases the formation of ettringite,

but when the $SiO_2/CaO$ ratio varies between 0.32 and 0.41 and the $Na_2O + K_2O/CaO$ ratio varies between 0.032 and 0.043, it promotes CSH formation to a certain extent. The replacement of 15% of cement with BFA decreased CSH formation by only 12%, whereas the replacement of 30% of cement with BFA decreased formation by up to 31%, compared to the control specimen. Through the replacement of up to 30% of the cement portion with BFA, the $Na_2O + K_2O/CaO$ ratio increased up to threefold (from 0.02 to 0.067) and maintained sufficient formation of calcium silicate hydrates (CSHs).

4. When there was extra alkalinity, namely, the $Na_2O + K_2O/CaO$ ratio in the cement matrix was not higher than 0.043, and the $SiO_2/CaO$ ratio varied in the range of 0.32–0.41, the concrete had a better structure, the highest density, better closed porosity, higher compressive strength, and can resists the highest number of freeze thaw cycles. Compared to the control samples, the compressive strength increased by up to 19.3% and the calculated number of freeze and thaw cycles increased to 51.5 and by 30% when 10–15% of cement was replaced with BFA.
5. It was found that expansion of the samples decreased with a higher amount of BFA in the mix. The lowest expansion of hardened mortar of 0.01% was observed after 56 days of storage of the samples in a 1 M NaOH solution at 80° C, when up to 30% of cement was substituted with BFA. The obtained results allow us to conclude that the substitution of cement with BFA suppresses the damaging ASR effect in sustainable concrete. High-alkali BFA has a beneficial effect on the development of new cementitious materials.
6. Several recommendations, based on the conducted research, may be presented to manufacturers:
   - Smaller BFA particles are more involved in the cement hydration process;
   - Higher-alkali-content BFA, due to the fact that hydration products fill concrete pores, has a positive effect on concrete's resistance to freeze–thaw cycles and ASR;
   - The possibility of increasing the amount of alkali in the different types of BFA may be considered in future research.

**Author Contributions:** Conceptualisation, D.N. and I.P.; methodology, D.N., I.P., L.K. and E.J.; investigation, D.N., I.P., L.K. and E.J.; resources, D.N., I.P., L.K. and E.J.; writing—original draft preparation, D.N., I.P., L.K. and E.J.; supervision, D.N., I.P., L.K. and E.J. All authors have read and agreed to the published version of the manuscript.

**Funding:** This research received no external funding.

**Data Availability Statement:** Data are contained within the article.

**Conflicts of Interest:** The authors declare no conflict of interest.

## References

1. Chaunsali, P.; Uvegi, H.; Osmundsen, R.; Laracy, M.; Poinot, T.; Ochsendorf, J.; Olivetti, E. Mineralogical and Microstructural Characterization of Biomass Ash Binder. *Cem. Concr. Compos.* **2018**, *89*, 41–51. [CrossRef]
2. International Energy Agency (IEA). *Key World Energy Statistics 2016*; IEA: Paris, France, 2016. [CrossRef]
3. Scurlock, J.M.O.; Hall, D.O. The Contribution of Biomass to Global Energy Use (1987). *Biomass* **1990**, *21*, 75–81. [CrossRef]
4. Odzijewicz, J.I.; Wołejko, E.; Wydro, U.; Wasil, M.; Jabłońska-Trypuć, A. Utilization of Ashes from Biomass Combustion. *Energies* **2022**, *15*, 9653. [CrossRef]
5. Wang, S.; Baxter, L. Comprehensive study of biomass fly ash in concrete: Strength, microscopy, kinetics and durability. *Fuel Process. Technol.* **2007**, *88*, 1165–1170. [CrossRef]
6. Rajamma, R.; Ball, R.J.; Tarelho, L.A.; Allen, G.C.; Labrincha, J.A.; Ferreira, V.M. Characterisation and use of biomass fly ash in cement-based materials. *J. Hazard. Mater.* **2009**, *172*, 1049–1060. [CrossRef]
7. Liu, Z.; Deng, P.; Zhang, Z. Application of silica-rich biomass ash solid waste in geopolymer preparation: A review. *Constr. Build. Mater.* **2022**, *356*, 129142. [CrossRef]
8. Tamanna, K.; Raman, S.N.; Jamil, M.; Hamid, R. Review Utilization of wood waste ash in construction technology: A review. *Constr. Build. Mater.* **2020**, *237*, 117654. [CrossRef]

9. Xiao, R.; Chen, X.; Wang, F.; Yu, G. The Physicochemical Properties of Different Biomass Ashes at Different Ashing Temperature. *Renew. Energy* **2011**, *36*, 244–249. [CrossRef]
10. Esteves, T.C.; Rajamma, R.; Soares, D.; Silva, A.S.; Ferreira, V.M.; Labrincha, J.A. Use of biomass fly ash for mitigation of alkali-silica reaction of cement mortars. *Constr. Build. Mater.* **2012**, *26*, 687–693. [CrossRef]
11. Gabrijel, I.; Jelčić Rukavina, M.; Štirmer, N. Influence of Wood Fly Ash on Concrete Properties through Filling Effect Mechanism. *Materials* **2021**, *14*, 7164. [CrossRef]
12. Ukrainczyk, N.; Vrbos, N.; Koenders, E.A.B. Reuse of Woody Biomass Ash Waste in Cementitious Materials. *Chem. Biochem. Eng. Q.* **2016**, *30*, 137–148. [CrossRef]
13. Wang, S.; Miller, A.; Llamazos, E.; Fonseca, F.; Baxter, L. Biomass fly ash in concrete: Mixture proportioning and mechanical properties. *Fuel* **2008**, *87*, 365–371. [CrossRef]
14. Maschio, S.; Tonello, G.; Piani, L.; Furlani, E. Fly and bottom ashes from biomass combustion as cement replacing components in mortars production: Rheological behaviour of the pastes and materials compression strength. *Chemosphere* **2011**, *85*, 666–671. [CrossRef] [PubMed]
15. Rissanen, J.; Ohenoja, K.; Kinnunen, P.; Illikainen, M. Partial Replacement of Portland-Composite Cement by Fluidized Bed Combustion Fly Ash. *J. Mater. Civ. Eng.* **2017**, *29*, 04017061. [CrossRef]
16. Rajamma, R.; Senff, L.; Ribeiro, M.; Labrincha, J.; Ball, R.; Allen, G.; Ferreira, V. Biomass fly ash effect on fresh and hardened state properties of cement based materials. *Compos. Part B Eng.* **2015**, *77*, 1–9. [CrossRef]
17. Berra, M.; Mangialardi, T.; Paolini, A.E. Reuse of woody biomass fly ash in cement-based materials. *Constr. Build. Mater.* **2015**, *76*, 286–296. [CrossRef]
18. Lazik, P.R.; Bošnjak, J.; Cetin, E.; Kücük, A. Application of wood ash as a substitute for fly ash and investigation of concrete properties. *Otto. Graf. J.* **2020**, *19*, 103–118.
19. Tulashie, S.K.; Dapaah, S.; Mensah, D.; Appiah, N. Palm fiber ash as a supplementary cementitious material for the production of mortar prism. *Innov. Infrastruct Solut.* **2021**, *7*, 3. [CrossRef]
20. Carević, I.; Štirmer, N.; Serdar, M.; Ukrainczyk, N. Effect of Wood Biomass Ash Storage on the Properties of Cement Composites. *Materials* **2021**, *14*, 1632. [CrossRef]
21. Udoeyo, F.F.; Inyang, H.; Young, D.T.; Oparadu, E.E. Potential of Wood Waste Ash as an Additive in Concrete. *J. Mater. Civ. Eng.* **2006**, *18*, 605–611. [CrossRef]
22. Ban, C.C.; Ramli, M. The Implementation of Wood Waste Ash as a Partial Cement Replacement Material in the Production of Structural Grade Concrete and Mortar: An Overview. *Resour. Conserv. Recycl.* **2011**, *55*, 669–685. [CrossRef]
23. Szcześniak, A.; Zychowicz, J.; Stolarski, A. Assessment of the Influence of Fly Ash Additive on the Tightness of Concrete with Furnace Cement CEM IIIA 32,5N. *Bull. Mil. Univ. Technol.* **2017**, *66*, 153–164. [CrossRef]
24. Wang, S.; Miller, A.; Llamazos, E.; Baxter, L.; Fonseca, F. Durability of Biomass Fly Ash Concrete: Freezing and Thawing and Rapid Chloride Permeability Tests. *Fuel* **2008**, *87*, 359–364. [CrossRef]
25. Teixeira, E.R.; Camões, A.; Branco, F.; Aguiar, J.; Fangueiro, R. Recycling of biomass and coal fly ash as cement replacement material and its effect on hydration and carbonation of concrete. *Waste Manag.* **2019**, *94*, 39–48. [CrossRef] [PubMed]
26. Demis, S.; Tapali, J.G.; Papadakis, V.G. An Investigation of the Effectiveness of the Utilization of Biomass Ashes as Pozzolanic Materials. *Constr. Build. Mater.* **2014**, *68*, 291–300. [CrossRef]
27. Romero, E.; Quirantes, M.; Nogales, R. Characterization of Biomass Ashes Produced at Different Temperatures from Olive-Oil-Industry and Greenhouse Vegetable Wastes. *Fuel* **2017**, *208*, 1–9. [CrossRef]
28. Rutkowska, G.; Wiśniewski, K.; Chalecki, M.; Górecka, M.; Miłosek, K. Influence of Fly-Ashes on Properties of Ordinary Concretes. *Ann. Wars. Univ. Life Sci. SGGW Land Reclam.* **2016**, *48*, 79–94. [CrossRef]
29. Popławski, J.; Lelusz, M. Utility assessment of biomass fly-ash for production of concrete products. *Czas. Technol.* **2017**, *2017*, 129–142. [CrossRef]
30. Thomas, M. *Optimizing the Use of Fly Ash in Concrete*; Portland Cement Association: Skokie, IL, USA, 2007; p. 5420.
31. Jaworska, B.; Stańczak, D.; Tarańska, J.; Jaworski, J. The Influence of Cement Substitution by Biomass Fly Ash on the Polymer–Cement Composites Properties. *Materials* **2021**, *14*, 3079. [CrossRef]
32. Pera, J.; Ambroise, J. Influence of different polymers on the properties of cementitious matrices. In Proceedings of the 10th International Congress on Polymers in Concrete—ICPIC'01, Honolulu, HI, USA, 21–24 May 2001.
33. Šantek Bajto, J.; Štirmer, N.; Cerković, S.; Carević, I.; Kostanić Jurić, K. Pilot Scale Production of Precast Concrete Elements with Wood Biomass Ash. *Materials* **2021**, *14*, 6578. [CrossRef]
34. Carević, I.; Baričević, A.; Štirmer, N.; Šantek Bajto, J. Correlation between physical and chemical properties of wood biomass ash and cement composites performances. *Constr. Build. Mater.* **2020**, *256*, 119450. [CrossRef]
35. Teker Ercan, E.E.; Andreas, L.; Cwirzen, A.; Habermehl-Cwirzen, K. Wood Ash as Sustainable Alternative Raw Material for the Production of Concrete—A Review. *Materials* **2023**, *16*, 2557. [CrossRef] [PubMed]
36. Tarelho, L.A.C.; Teixeira, E.R.; Silva, D.F.R.; Modolo, R.C.E.; Labrincha, J.A.; Rocha, F. Characteristics of distinct ash flows in a biomass thermal power plant with bubbling fluidised bed combustor. *Energy* **2015**, *90*, 387–402. [CrossRef]
37. *LST EN 197-1:2011*; Cement—Part 1: Composition, Specifications and Conformity Criteria for Common Cements. The National Standards Authority of Ireland (NSAI): Dublin, Ireland, 2011.

38. Lothenbach, B.; Scrivener, K.; Hooton, R.D. Supplementary cementitious materials. *Cem. Concr. Res.* **2011**, *41*, 1244–1256. [CrossRef]
39. *LST EN 12620:2003+A1:2008*; Aggregates for Concrete. Lithuanian Standards Board: Vilnius, Lithuania, 2008.
40. *LST EN 12350-5:2019*; Testing Fresh Concrete—Part 5: Flow Table Test. Lithuanian Standards Board: Vilnius, Lithuania, 2019.
41. *LST EN 12390-7:2019;* Testing Hardened Concrete—Part 7: Density of Hardened Concrete. Lithuanian Standards Board: Vilnius, Lithuania, 2019.
42. *LST EN 12390-3:2019;* Testing Hardened Concrete—Part 3: Compressive Strength of Test Specimens. Lithuanian Standards Board: Vilnius, Lithuania, 2019.
43. *LST EN 12390-5:2019;* Testing Hardened Concrete—Part 5: Flexural Strength of Test Specimens. Lithuanian Standards Board: Vilnius, Lithuania, 2019.
44. *LST EN 12504-4*; Testing concrete—Part 4: Determination of Ultrasonic Pulse Velocity. Lithuanian Standards Board: Vilnius, Lithuania, 2019.
45. Scheikin, A.E.; Dopschic, L.M. *Cement Concrete with High Frost Resistance*; Stroyizdat: Leningrad, Russia, 1989.
46. Cabrera, M.; Galvin, A.P.; Agrela, F.; Carvajal, M.D.; Ayuso, J. Characterisation and technical feasibility of using biomass bottom ash for civil infrastructures. *Constr. Build. Mater.* **2014**, *58*, 234–244. [CrossRef]
47. Fořt, J.; Šál, J.; Ševčík, R.; Doleželová, M.; Keppert, M.; Miloš, J.; Záleská, M.; Stehel, V.; Černý, R. Biomass fly ash as an alternative to coal fly ash in blended cements: Functional aspects. *Constr. Build. Mater.* **2021**, *271*, 121544. [CrossRef]
48. Rissanen, J.; Giosué, C.; Ohenoja, K.; Kinnunen, P.; Marcellini, M.; Letizia Ruello, M.; Tittarelli, F.; Illikainen, M. The effect of peat and wood fly ash on the porosity of mortar. *Constr. Build. Mater.* **2019**, *223*, 421–430. [CrossRef]
49. Quarcioni, V.A.; Chotoli, F.F.; Coelho, A.C.V.; Cintotto, M.A. Indirect and direct Chapelle's method for the determination of lime consumption in pozzolanic materials. *IBRACON Struct. Mater.* **2015**, *8*, 1–7. [CrossRef]
50. Mitchell, L.D.; Margeson, J.C. The effects of solvents on CSH as determined by thermal analysis. *J. Therm. Anal. Calorim.* **2006**, *86*, 591–594. [CrossRef]
51. Berodier, E.; Scrivener, K. Understanding the Filler Effect on the Nucleation and Growth of C–S–H. *J. Am. Ceram. Soc.* **2014**, *97*, 3764–3773. [CrossRef]
52. Shehata, M.H.; Thomas, M.D. Use of ternary blends containing silica fume and fly ash to suppress expansion due to alkali–silica reaction in concrete. *Cem. Concr. Res.* **2002**, *32*, 341–349. [CrossRef]
53. Aquino, W.; Lange, D.A.; Olek, J. The influence of metakaolin and silica fume on the chemistry of alkali–silica reaction products. *Cem. Concr. Compos.* **2001**, *23*, 485–493. [CrossRef]
54. Karim, M.R.; Zain, M.F.M.; Jamil, M.; Lai, F.C. Fabrication of a non-cement binder using slag, palm oil fuel ash and rice husk ash with sodium hydroxide. *Constr. Build. Mater.* **2013**, *49*, 894–902. [CrossRef]
55. Jaturapitakkul, C.; Tangpagasit, J.; Songmue, S.; Kiattikomol, K. Filler effect and pozzolanic reaction of ground palm oil fuel ash. *Constr. Build. Mater.* **2011**, *25*, 4287–4293. [CrossRef]
56. Kaminskas, R.; Barauskas, I.; Kubiliute, R.; Monstvilaite, D. The effect of the pozzolanic activity of different micro-fillers on portland cement hydration. *Ceram. Silikáty* **2020**, *64*, 145–154. [CrossRef]
57. Thomas, H.F.W. *Cement Chemistry*, 2nd ed.; Thomas Telford Publishing: London, UK, 1997.
58. Jiahui, P.; Jianxin, Z.; Jindong, Q. The mechanism of the formation and transformation of ettringite. *J. Wuhan Univ. Technol. Mat. Sci. Edit.* **2006**, *21*, 158–161. [CrossRef]
59. Prince, W.; Espagne, M.; Aitcin, P.C. Ettringite formation: A crucial step in cement superplasticizer compatibility. *Cem. Concr. Res.* **2003**, *33*, 635–641. [CrossRef]
60. Palou, M.T.; Kuzielova, E.; Novotny, R.; Šoukal, F.; Žemlička, M. Blended cements consisting of Portland cement–slag–silica fume–metakaolin system. *J. Therm. Anal. Calorim.* **2016**, *125*, 1025–1034. [CrossRef]
61. Wang, Y.; Shui, Z.; Wang, L.; Gao, X.; Huang, Y.; Song, Q.; Liu, K. Alumina-rich pozzolan modification on Portland-limestone cement concrete: Hydration kinetics, formation of hydrates and long-term performance evolution. *Constr. Build. Mater.* **2020**, *258*, 119712. [CrossRef]
62. Pocius, E.; Nagrockienė, D.; Pundienė, I. The influence of concrete sludge from residual concrete on fresh and hardened cement paste properties. *Materials* **2023**, *16*, 2531. [CrossRef]
63. Shin, S.M.; Ho, C.S.; Song, Y.S.; Lin, J.P. Kinetics of the Reaction of $Ca(OH)_2$ with $CO_2$ at Low Temperature. *Ind. Eng. Chem. Res.* **1999**, *38*, 1316–1322. [CrossRef]
64. Elinwa, A.U.; Mahmood, Y.A. Ash from timber waste as cement replacement material. *Cem. Concr. Compos.* **2002**, *24*, 219–222. [CrossRef]
65. Elinwa, A.U.; Ejeh, S.P. Effects of incorporation of sawdust incineration fly ash in cement pastes and mortars. *J. Asian Archit. Build. Eng.* **2004**, *3*, 1–7. [CrossRef]
66. Vaičiukynienė, D.; Balevičius, G.; Vaičiukynas, V.; Kantautas, A.; Jakevičius, L. Synergic effect between two pozzolans: Clinoptilolite and silica gel by-product in a ternary blend of a Portland cement system. *Const. Build. Mater.* **2022**, *344*, 128155. [CrossRef]
67. Schöler, A.; Lothenbach, B.; Winnefeld, F.; Haha, M.B.; Zajac, M.; Ludwig, H.M. Early hydration of SCMblended Portland cements: A pore solution and isothermal calorimetry study. *Cem. Concr. Res.* **2017**, *93*, 71–82. [CrossRef]

68. Johnson, A.; Catalan, L.; Kinrade, S. Characterization and evaluation of fly-ash from co-combustion of lignite and wood pellets for use as cement admixture. *Fuel* **2010**, *89*, 3042–3050. [CrossRef]
69. Feng, C.; Roels, S.; Janssen, H. Towards a more representative assessment of frost damage to porous building materials. *Build. Environ.* **2019**, *164*, 106343. [CrossRef]
70. Koroth, S.R. *Evaluation and Improvement of Frost Durability of Clay Bricks*; Concordia University: Montreal, QC, Canada, 1997.
71. Liu, L.; Wang, X.; Zhou, J.; Chu, H.; Shen, D.; Chen, H.; Qin, S. Investigation of pore structure and mechanical property of cement paste subjected to the coupled action of freezing/thawing and calcium leaching. *Cem. Concr. Res.* **2018**, *109*, 133–146. [CrossRef]
72. Omran, A.; Soliman, N.; Xie, A.; Davidenko, T.; Tagnit-Hamou, A. Field trials with concrete incorporating biomass-fly ash. *Const. Build. Mater.* **2018**, *186*, 660–669. [CrossRef]
73. Zhu, H.; Zhai, M.; Liang, G.; Li, H.; Wu, Q.; Zhang, C.; Hua, S. Experimental study on the freezing resistance and microstructure of alkali-activated slag in the presence of rice husk ash. *J. Build. Eng.* **2021**, *38*, 102173. [CrossRef]
74. Teixeira, E.R.; Camões, A.; Branco, F.G. Valorisation of wood fly ash on concrete. *Resour. Conserv. Recycl.* **2019**, *145*, 292–310. [CrossRef]
75. Nagrockienė, D.; Daugėla, A. Investigation into the properties of concrete modified with biomass combustion fly ash. *Constr. Build. Mater.* **2018**, *174*, 369–375. [CrossRef]
76. Wang, S. Cofired biomass fly ashes in mortar: Reduction of Alkali Silica Reaction (ASR) expansion, pore solution chemistry and the effects on compressive strength. *Constr. Build. Mater.* **2015**, *82*, 123–132. [CrossRef]